Title

Adsorption Behavior of a Cyano-Functionalized Porphyrin on Cu(111) and Ag(111): From Molecular Wires to Ordered Supramolecular Two-Dimensional Aggregates

Journal

The Journal of Physical Chemistry C, 121(47)

ISSN

1932-7447

Authors

Lepper, Michael
Schmitt, Tobias
Gurrath, Martin
et al.

Publication Date

2017-11-30

DOI

10.1021/acs.jpcc.7b08382

Peer reviewed

THE JOURNAL OF PHYSICAL CHEMISTRY C

Article

Cite This: J. Phys. Chem. C 2017, 121, 26361-26371

pubs.acs.org/JPCC

Adsorption Behavior of a Cyano-Functionalized Porphyrin on Cu(111) and Ag(111): From Molecular Wires to Ordered Supramolecular Two-Dimensional Aggregates

Michael Lepper,[†,‡] Tobias Schmitt,[§] Martin Gurrath,[‡,∥] Marco Raschmann,[§] Liang Zhang,[†,‡] Michael Stark,[†,‡] Helen Hölzel,[‡,⊥] Norbert Jux,[‡,⊥] Bernd Meyer,[‡,∥] M. Alexander Schneider,[§] Hans-Peter Steinrück,[†,‡] and Hubertus Marbach*[,†,‡]

[†]Lehrstuhl für Physikalische Chemie II, Universität Erlangen-Nürnberg, Egerlandstr. 3, 91058 Erlangen, Germany

[‡]Interdisciplinary Center for Molecular Materials (ICMM), Universität Erlangen-Nürnberg, Henkestr. 42, 91054 Erlangen, Germany

[§]Lehrstuhl für Festkörperphysik, Universität Erlangen-Nürnberg, Staudtstr. 7, 91058 Erlangen, Germany

[∥]Computer-Chemistry-Center (CCC), Universität Erlangen-Nürnberg, Nägelsbachstr. 25, 91052 Erlangen, Germany

[⊥]Lehrstuhl für Organische Chemie II, Universität Erlangen-Nürnberg, Henkestr. 42, 91054 Erlangen, Germany

Supporting Information

ABSTRACT: We investigate the impact of peripheral cyano functionalization of the previously well-studied 2*H*-tetraphenylporphyrin (2HTPP) by scanning tunneling microscopy (STM) and density functional theory (DFT). The adsorption behavior of 2*H*-tetrakis(*p*-cyano)-phenylporphyrin (2HTCNPP) is studied at room temperature and at 80 K on Cu(111) and Ag(111). Interestingly, the cyano-functionalized porphyrins tend to form isolated 1D chains on Cu(111), in particular after mild annealing at 350 K. The individual 2HTCNPPs as well as the formed chains are oriented along the main crystallographic directions of the Cu(111) substrate due to a strongly attractive and site-specific interaction between the iminic nitrogens of the 2HTCNPP and Cu substrate atoms. The linking within the 1D molecular chains is realized by Cu adatoms as evidenced by comparison of STM and DFT. In contrast, on Ag(111) the molecules assemble into 2D supramolecular layers with long-range order and a square unit cell, stabilized by molecule−molecule interactions. The orientation of the molecules with respect to the unit cell lattice vectors leads to organizational chirality. By codeposition of cobalt, the porphyrin molecules are metalated at room temperature. We did not observe any evidence for metal−organic network formation on Ag(111), even after varying the deposition parameters or the order of metal and porphyrin deposition. Our study shows that cyano functionalization of porphyrins can give rise to novel and unique self-assembled structures like 1D molecular chains without any cross-connections via adatom linking.

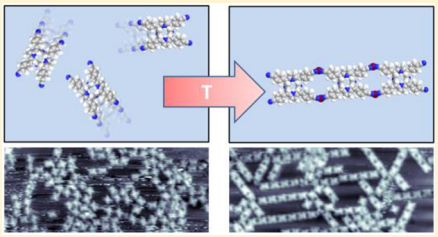

INTRODUCTION

The bottom-up design and construction of nanoscale architectures has become an active research area in surface science due to the growing demand for miniaturization of functional building blocks.[1−3] The self-assembly of organic molecules on metal surfaces is a powerful route toward the fabrication of such nanodevices. Utilizing specific adsorption behaviors and a controlled interplay of adsorbate−substrate and adsorbate−adsorbate interactions allows for creating novel materials with outstanding properties.[4−6] Porphyrins are an especially promising class of functional molecules since they offer inherent conformational flexibility, reactivity, and useful electronic properties.[6−9] Depending on the combination of substrate and porphyrin derivative, a variety of characteristic adsorption behaviors have been reported.[10−21] Two key factors, which determine the resulting properties, are adsorbate−substrate and adsorbate−adsorbate interactions. As an example, the difference in adsorbate−substrate interactions leads to completely different adsorption behaviors of free-base tetraphenylporphyrin (2HTPP) on Cu(111) and on Ag(111) at room temperature (RT).[15,22−24] At low to intermediate coverages, individual molecules are observed on Cu(111). The molecules are aligned and diffuse along one of the three main crystallographic directions of the substrate.[16,22,23,25] This behavior is attributed to strong molecule−substrate interactions due to a site-specific bond formation of the nonterminated iminic nitrogen atoms of the free-base porphyrin with Cu substrate atoms, leading to a tilt of the associated pyrrole rings into an upright orientation perpendicular to the surface.[16,22,23,25] On the other hand, on Ag(111) 2HTPP forms supramolecular arrangements with a square unit cell. Due to weaker and less site-specific adsorbate−substrate interactions between the iminic nitrogens and the Ag surface, T-type intermolecular interactions between the phenyl rings of

Received: August 22, 2017
Revised: October 19, 2017
Published: November 1, 2017

DOI: 10.1021/acs.jpcc.7b08382
J. Phys. Chem. C 2017, 121, 26361−26371

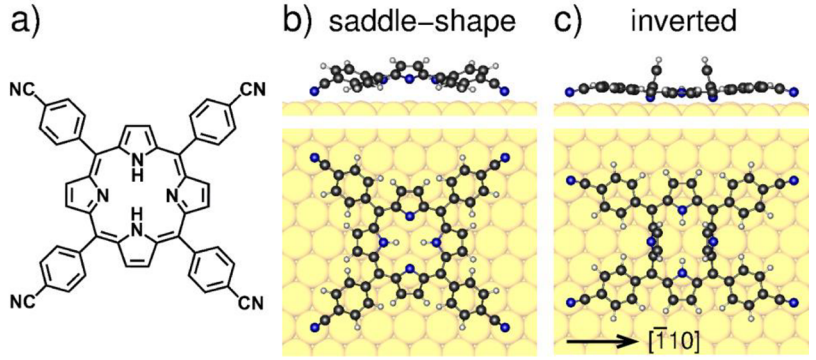

Figure 1. (a) Scheme of 2HTCNPP. Side and top view of the DFT-optimized (b) saddle-shape and (c) inverted conformation of 2HTCNPP on Cu(111). Cu, C, N, and H atoms are shown in yellow, dark gray, blue, and white, respectively.

neighboring molecules are proposed to dominate the observed adsorption behavior.[15]

In addition to exploiting T-type, π-type, and van der Waals adsorbate−adsorbate interactions, a promising strategy for the controlled generation of molecular architectures on metal surfaces is the formation of so-called metal−organic networks. Thereby, in contrast to the conventional self-assembly of supramolecular arrangements, the intermolecular interactions are realized by the interstitial coordination of metal atoms, which can be achieved in quite different ways. Villagomez et al. reported a direct coordination of carbon atoms of the organic molecule to Cu adatoms, enabling the formation of chain-like "wagon trains" on Cu(111).[26] A similar bonding motif was utilized by Haq et al. to construct organometallic wires as well as two-dimensional networks on Cu(110).[27] Due to the robust nature of these bonding motifs, such structures of periodically ordered building blocks can be stable even at room temperature.[28,29]

Coordination via metal linkers can also be targeted and realized by introducing functional groups in the organic molecules. The carboxylic group is one of the essential subunits in organic chemistry, which can be used to induce network structures. Several publications report the coordination of negatively polarized oxygen atoms of carboxylic groups and positively polarized metal atoms.[30−32] Another important route in network surface chemistry is the coordination of nitrogen-terminated molecules. The metal atoms required to form networks are provided either by the surface[33] or by deposition.[34,35] El Garah et al. reported the linking of porphyrins with Co on HOPG in solution, highlighting the stability of such network structures.[36] The importance of the choice of the metal substrate for such network formation was shown for pyridyl-porphyrins on different substrates.[11,37] While on Cu(111) network formation is observed, no such linking is found on Ag(111).[11,37,38] Among nitrogen-terminated species, molecules with peripheral cyano groups are of great interest. Besides the possibility to form metal-linked networks,[28,38−43] the cyano groups also enable intermolecular interactions between hydrogen bonding and dipolar coupling.[41,44−48]

To fully describe network formation on metal surfaces, one has to understand the interplay of molecule−molecule interactions, molecule−substrate interactions, and metal coordination.[28,34,40,44,47] In our present study, we investigate this complex balance by studying the adsorption behavior of a porphyrin terminated by four cyano groups adsorbed on two different substrates, namely, Cu(111) and Ag(111). Figure 1a depicts the chemical structure of the investigated 2*H*-tetrakis(*p*-cyano)-phenylporphyrin (2HTCNPP). In the gas phase and also on most substrates, e.g., Ag(111), porphyrins adopt the so-called "saddle-shape" conformation (see Figure 1b).[10,14,49] This conformation was also initially proposed for free-base tetraphenylporphyrins on Cu(111).[22,50,51] However, very recently it was shown that 2HTCNPP and the closely related 2HTPP undergo large structural changes upon adsorption on Cu(111) due to the strong interaction between Cu and the iminic nitrogens, resulting in a particular, strongly distorted "inverted" conformation (see Figure 1c). This peculiar interaction is expected to be not present on the less reactive Ag(111) surface. We investigate and compare the adsorption behavior of 2HTCNPP on both surfaces with scanning tunneling microscopy (STM). In addition, density functional theory (DFT) calculations were performed to achieve a detailed understanding of the peculiar formation of 1D molecular chains of the latter porphyrin derivative on Cu(111).

METHODS SECTION

The experiments and sample preparations were performed in two different ultrahigh vacuum (UHV) systems at a background pressure in the low 10^{-10} mbar regime. The first houses a variable-temperature scanning tunneling microscope (STM), namely, a RHK UHV VT STM 300 operated at RT with a RHK SPM 1000 electronics. The second is a home-built LT-STM enabling measurements at 80 K. All STM images were acquired in constant current mode, with a Pt/Ir tip (RT-STM) or etched W tip (LT-STM), and the bias voltage was applied to the sample. The STM images were processed with the WSxM software,[52] and moderate filtering (Gaussian smoothing, background subtraction) was applied for noise reduction. The preparation of the clean Cu(111) and Ag(111) surfaces was done by repeated cycles of Ar^+ sputtering (500 eV) and annealing to 850 K. The 2HTCNPP molecules were deposited onto the metal substrates held at RT by thermal sublimation from a home-built Knudsen cell at 340 °C. The coverages of the full 2HTCNPP layer on Ag(111) were determined by STM and correspond to 0.033 ML; thereby, 1 ML is defined as one adsorbate molecule per substrate surface atom. The ⟨1̄10⟩ axes of Cu(111) were determined either directly by imaging the densely packed Cu rows at 80 K or by codeposition of 2HTPP on Cu(111); the azimuthal orientation of 2HTPP is known to coincide with the main crystallographic directions of Cu(111) at RT.[16] Co and Ni deposition onto the metal substrates held at RT was carried out with a Focus EFM 3 electron beam evaporator.

DOI: 10.1021/acs.jpcc.7b08382
J. Phys. Chem. C 2017, 121, 26361−26371

The DFT calculations were performed with the periodic plane wave code PWscf of the Quantum Espresso software package,[53] using the Perdew–Burke–Ernzerhof (PBE) exchange-correlation functional,[54] Grimme D3 van der Waals corrections with Becke–Johnson damping,[55,56] Vanderbilt ultrasoft pseudopotentials,[57] and a plane-wave cutoff energy of 30 Ry. Surface structures were represented by periodically repeated slabs with a thickness of three layers and a hexagonal (10 × 10) surface unit cell for the calculations of isolated, noninteracting molecules (300 Cu atoms in total). The calculated PBE bulk lattice constant of Cu of 3.632 Å was chosen for the lateral extensions of the slabs. The atoms in the bottom layer were kept fixed, and only the two upper layers together with the adsorbate were allowed to relax in the geometry optimizations using a force convergence threshold of 3 meV/Å. A (2,2,1) Monkhorst–Pack *k*-point mesh together with a Gaussian smearing with a smearing width of 0.02 Ry were mandatory for getting converged adsorption energies.[58] Molecule–molecule interactions were probed by reducing the size of the surface unit cell to (8 × 10) and (7 × 10). The density of the *k*-point mesh was then increased to (3, 2, 1). STM images were calculated in the Tersoff–Hamann approximation in the constant current mode with a density iso-contour value of 10^{-6} e/bohr^3 using our own postprocessing code.[59]

All chemicals were purchased from Sigma-Aldrich, Acros Organics, Fluka, Fisher Scientific, or Alfa Aesar and used without further purification. Pyrrole and solvents for chromatography were distilled prior to usage. Dichloromethane was distilled from K_2CO_3. Microwave-assisted reactions were carried out in a Biotage initiator + monomode microwave reactor and its respective vials. The standard stirring rate was 600 rpm, fixed hold time (FHT) was on, and no external cooling was applied.

The 2HTCNPP was synthesized according to a modified literature procedure[60] which was carried out twice: a 20 mL μW-vial was charged with *p*-cyanobenzaldehyde (0.263 g, 2.00 mmol), pyrrole (140 μL, 2.00 mmol), and CH_2Cl_2 (20 mL). Iodine (0.050 g, 0.197 mmol) was added as solid, and the vial was sealed. The mixture was stirred in the μW for 5 min at 40 °C (absorption level: low, prestirring: 20 s, Pmax = 100 W). After the reaction was completed, *p*-chloranil (0.368 g, 1.50 mmol) was added carefully, and the vial was sealed again. The mixture was stirred in the μW for 1 min at 40 °C (absorption level: low, prestirring: 20 s, P_{max} = 100 W).

The two batches were combined, and the solvent was removed under reduced pressure. The crude product was prepurified by plug filtration (SiO_2, diameter: 10 cm, length: 6 cm, CH_2Cl_2:EtOAc = 30:1). The solvent was removed under reduced pressure, and final purification was achieved by column chromatography (SiO_2, diameter: 6.5 cm, length: 20 cm, CH_2Cl_2), yielding the product as a purple solid in 46% (0.329 g, 0.460 mmol).

The 2HTCNPP was fully characterized, including ^{1}H NMR, ^{13}C NMR, UV/vis spectroscopies, and mass spectroscopy. All obtained data were in accord with those known in the literature and were fully consistent with the structure of the porphyrin.[61]

RESULTS AND DISCUSSION

2HTCNPP/Cu(111). The STM images for 2HTCNPP on Cu(111) prepared at room temperature are shown in Figure 2, with a coverage of 0.008 ML. The STM images were taken at 80 K and RT, respectively. We observe loosely organized

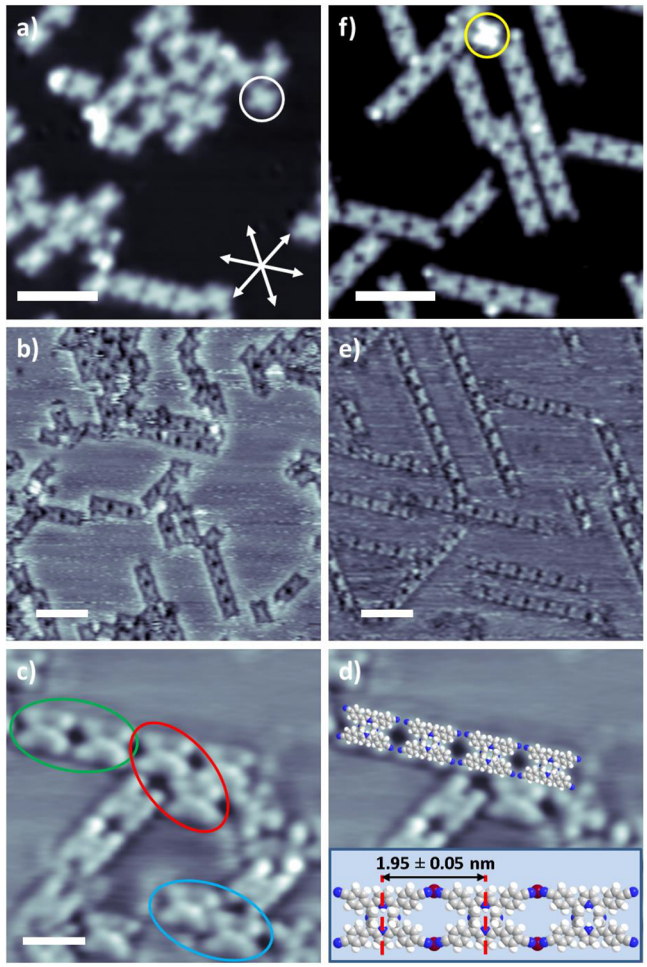

Figure 2. 2HTCNPP deposited on Cu(111) at RT: (a) measured at 80 K (U_{bias} = −1.50 V, I_{set} = 0.1 nA, scale bar = 5 nm); (b) measured at RT (U_{bias} = −0.90 V, I_{set} = 30 pA, scale bar = 5 nm); (c) measured at RT at an enlarged scale, illustrating the three different interaction motifs that can be found: hydrogen bonds (red circle), dipolar coupling (blue circle), and one-dimensional chains (green circle) (U_{bias} = −0.90 V, I_{set} = 30 pA, scale bar = 2 nm); (d) as (c) but overlaid with a molecular model; the inset shows the arrangement of molecules and linking adatoms; (e) after heating to 350 K, measured at RT (U_{bias} = −0.84 V, I_{set} = 29 pA, scale bar = 5 nm); (f) after heating to 423 K, measured at 80 K (U_{bias} = −2.0 V, I_{set} = 0.1 nA, scale bar = 5 nm), and one metalated molecule is marked by a yellow circle.

agglomerates, which—especially for the experiments conducted solely at room temperature—are dominated by short chains with a length of up to four molecules. Also other arrangements and isolated molecules are observed as indicated in Figure 2a–c. Notably, all molecules are aligned along one of the three $\langle\bar{1}10\rangle$ azimuths, that is, the densely packed Cu rows of the Cu(111) surface. At RT, diffusion of the individual isolated molecules along these main crystallographic directions is observed (see Figure S1 in the Supporting Information), similar to the results of 2HTPP on Cu(111).[16,22]

Before addressing the molecular interactions, we discuss the appearance of the individual 2HTCNPPs. The molecules predominantly appear as four bright lobes in the periphery and two dominating protrusions in the center with an overall elongated rectangular shape as seen in Figure 3e,f and also Figure 2c. Considering the chemical structure of 2HTCNPP shown in Figure 1a, the peripheral lobes are attributed to the

DOI: 10.1021/acs.jpcc.7b08382
J. Phys. Chem. C 2017, 121, 26361–26371

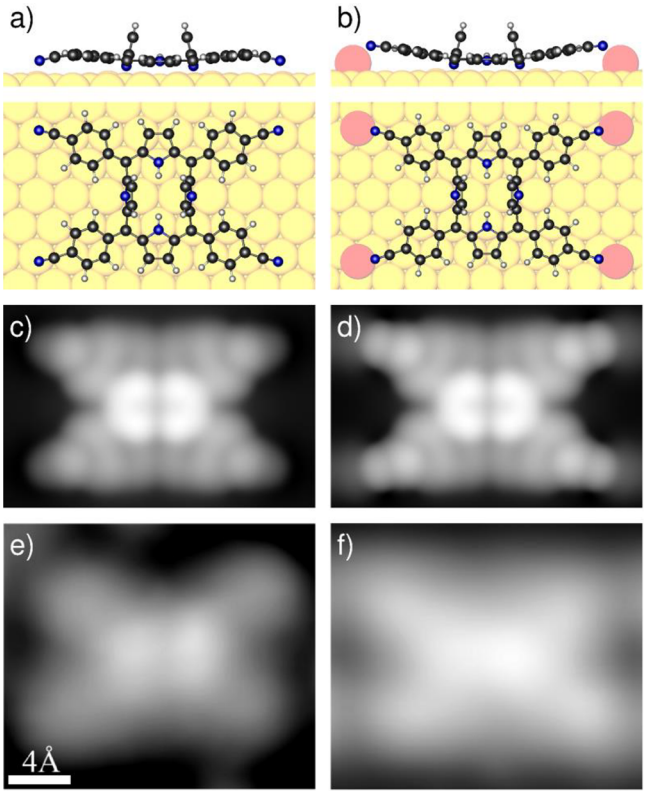

Figure 3. Side and top view of the DFT-optimized inverted structure of 2HTCNPP adsorbed on Cu(111) (a) without and (b) with additional Cu adatoms. (c,d) Corresponding calculated STM images for a bias voltage of U_{bias} = −1.0 V. (e) High-resolution image of an individual 2HTCNPP molecule measured at 80 K (U_{bias} = −1.50 V, I_{set} = 0.1 nA). The corresponding molecule is indicated with a white circle in Figure 2a. (f) High-resolution image of a 2HTCNPP molecule that is part of a linear chain measured at 80 K after heating the sample to 423 K (U_{bias} = −2.0 V, I_{set} = 0.1 nA).

phenyl legs, which are known to dominate the appearance of porphyrins on metal substrates.[7,8,14,47,62,63] In previous reports on the similar 2HTPP molecule on Cu(111), a saddle-shape conformation of the adsorbed porphyrin was postulated.[22,51] However, just very recently the very peculiar "inverted" structure as shown in Figure 1c was identified, which is characterized by a coordination of the two iminic nitrogen atoms to the Cu(111) surface via their lone electron pairs. The corresponding two pyrrole rings are strongly tilted, that is, they enclose approximately a right angle with the surface. The other two pyrrole rings and the peripheral phenyl rings are almost parallel to the surface.[23,25] The position and distance of the two bright spots observed in the center of the molecule fit to two opposing upward bent pyrrole groups. The molecular axis given by the two central protrusions is always aligned along one of the three main crystallographic directions of the Cu(111) surface, which is a result of the strong coordinative bond of the iminic nitrogen atoms with the Cu substrate atoms.[10,23−25,37] The upward tilted pyrrole rings give room for the two phenyl rings to move away from the horizontal pyrrole rings and bind with their CN group to the substrate causing the distinctly rectangular shape of the molecule.

We next address the different molecule−molecule interaction motifs found for room-temperature deposition in Figure 2a−c. The motifs marked with blue and red can be interpreted as due to hydrogen bonds or dipolar couplings, respectively, which are known to be typical interaction motifs for cyano linkers.[40,41,44−48] As a third and overall dominating motif after annealing, short 1D chain structures can be found, marked in green. Since all molecules are imaged with the same appearance in STM, it can be concluded that the intramolecular conformations are unaffected by the corresponding interaction motif occurring at the periphery of the 2HTCNPPs.

Interestingly, after mild annealing to 350 K for 10 min, the spatial organization of the molecules significantly increases (see Figure 2e). The vast majority of molecules is now arranged in chains oriented along one of the three densely packed substrate directions. Annealing to 423 K does not increase the chain length but leads to a change of the appearance of some molecules (marked yellow) in the STM images at 80 K in Figure 2f. This behavior is attributed to a chemical reaction, that is, the so-called self-metalation of 2HTCNPP with Cu atoms from the Cu(111) substrate, yielding CuTCNPP.[18,63,64] On Cu(111), metalated molecules are known to have a different appearance in STM[63] and are also much more mobile than their free-base analogues.[16,65] These observations are due to a lifting of the highly attractive interaction of the iminic nitrogens with the substrate, which results in a significant change of the intramolecular conformation. The few metalated molecules are not attached to the chains anymore (see also Figure S2 in the Supporting Information). The detaching of CuTCNPPs could be due to the different conformation that might not "fit" to the existing chains.

Notably, for 2HTCNPP molecules no attachment or detachment of molecules to/from the chains was observed at RT, suggesting sufficient lateral stabilization of the molecules within the chain. In addition, no long-range 2D order was observed even at coverages close to one closed layer of molecules (see Figure S2 in the Supporting Information). The formation of the linear chains is clearly a thermally activated process. When molecules are deposited at RT, the process is slow but possible. This we conclude from the more frequent appearance of chains in the RT measurements where the sample was kept at RT for hours compared to the samples measured at 80 K which were quenched to below 200 K within 10 min.

To further analyze the formation of 2HTCNPP chains on Cu(111), a close up of the surface after deposition at room temperature is presented in Figure 2c. It shows a chain consisting of four 2HTCNPP molecules. In Figure 2d, the STM image is overlaid with models of 2HTCNPP. The alignment of the molecules along one of the main crystallographic directions leads to an arrangement in which the cyano groups of neighboring chain molecules face each other head-to-head. Considering the polarity of the cyano groups, one expects a repulsive interaction for this local arrangement. Furthermore, a head-to-head orientation of the molecules combined with the relatively large distance of peripheral groups is not in line with commonly observed T-type and $\pi-\pi$ intermolecular interaction motifs of porphyrins.[17,66,67] For the same reasons, also the known interactions for cyano groups, namely, via hydrogen bonds and dipolar coupling, can be ruled out.[40,41,44−48]

To identify the linking mechanism and the driving force for the linear chain formation, we performed a series of DFT calculations. We started by determining the adsorption geometry of single, well-separated 2HTCNPP molecules in a large (10 × 10) surface unit cell. Six different conformations of the porphyrin molecule on the Cu(111) surface were considered: the conventional saddle shape (Figure 1b) with

DOI: 10.1021/acs.jpcc.7b08382
J. Phys. Chem. C 2017, 121, 26361−26371

the inner H atoms of the macrocycle pointing away from the surface, an upside-down saddle shape in which the H atoms point toward the surface, and the inverted structure (Figure 1c), all of them with the NH···HN axis either oriented parallel or perpendicular to the close-packed ⟨$\bar{1}$10⟩ Cu rows (see the Supporting Information for more details).

As for nonfunctionalized 2HTPP,[23] we find that the inverted structure with the hydrogens perpendicular to the close-packed Cu rows is the energetically most favorable configuration of 2HTCNPP on Cu(111) (see Figure 1c). This structure is lower in energy by 0.54 eV than the commonly assumed saddle-shape geometry in its lowest-energy orientation, in which the hydrogens are aligned parallel to the Cu rows (see Figure 1b). Interestingly, the second-best structure is the upside-down saddle-shape structure, which has not been considered before. The structure of the porphyrin core in the inverted 2HTCNPP configuration is very similar to that found previously for the nonfunctionalized 2HTPP.[23] The iminic nitrogen atoms of the upright-standing pyrrole rings are in a bridging position between two surface Cu atoms with a Cu−N distance of only 2.13 Å. The additional CN groups, however, have a clear impact on the orientation of the phenyl rings and the overall shape of the porphyrin molecule (see Figure 1c). The peripheral cyano groups bend down toward the surface, and the N atoms have a strong preference to bind on top of a surface Cu atom. Indeed, by using HCN as a test molecule in our DFT calculations to probe the strength of the surface−cyano interaction, we find that only the Cu on-top position is attractive, whereas all other sites are repulsive (with the dispersion correction turned off). Because of the preferred Cu on-top position of the cyano nitrogen atoms, the porphyrin molecule adjusts to the lattice parameters of the Cu(111) surface, which leads to a slight elongation of its shape, which pronounces the rectangular distortion of the porphyrin molecules in the inverted configuration.[23,25] This finding is in line with the experimental STM data, in which the 2HTCNPP indeed appears elongated in the direction of the axis of the two iminic nitrogen atoms, i.e., one of the close-packed directions of the Cu atoms, as mentioned above. The attractive Cu−N interaction of the cyano end group increases the porphyrin binding energy by about 0.5 eV compared to nonfunctionalized 2HTPP.

Furthermore, the Cu atoms underneath the cyano nitrogen atoms are pulled out of the surface by about 0.15 Å. Such a lifting of the surface Cu atoms through the interaction with cyano groups has been reported before for TCNQ adsorbed on Cu(100).[68] In this study it was claimed that the lifting of the Cu atoms creates a stress field in such a way that the energy cost for lifting a neighboring Cu atom is reduced, which makes it more favorable for the next molecule to adsorb at this site.[68] Thus, an effective substrate-mediated adsorbate−adsorbate attraction is introduced, which can have a profound effect on the molecular self-assembly. To probe whether this mechanism could be responsible for the observed chain formation of the 2HTCNPP molecules, we reduced the size of our supercell to bring the CN groups closer together and calculated the change in the porphyrin binding energy. In the (10 × 10) supercell the CN groups of the periodically repeated images are separated by four Cu−Cu distances (three Cu−Cu distances for the inverted porphyrin geometry, see Figure 4a). For the smaller supercells, in which the CN groups coordinate to neighboring Cu atoms (see Figure 4b,c) or in which they are only two Cu−Cu distances apart (not shown), we find a slightly reduced porphyrin binding energy. Although the small change reported in Figure 4c is well within the numerical uncertainty of our *k*-point sampling, overall the results indicate a repulsive but not an attractive interaction between the cyano-functionalized porphyrin molecules.

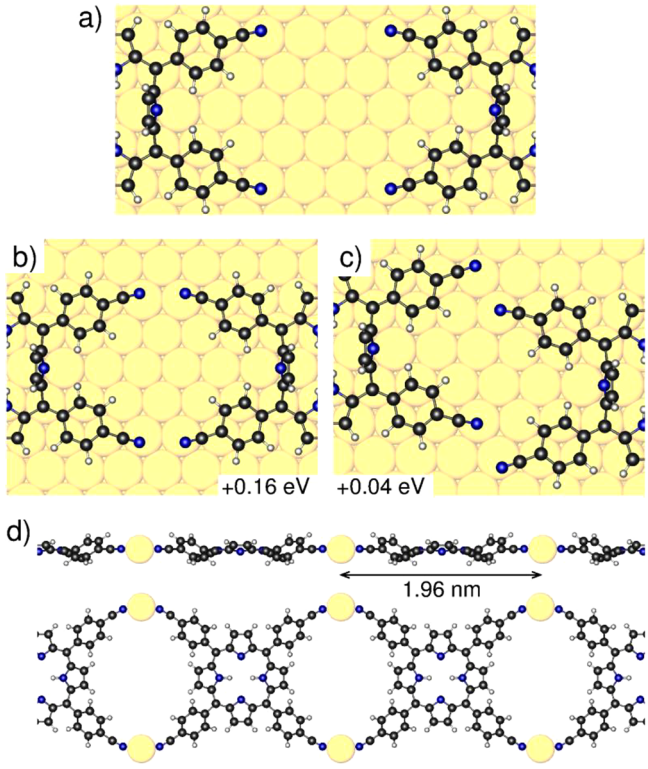

Figure 4. (a) Relative position of the peripheral cyano groups of the periodic 2HTCNPP images in the (10 × 10) supercell calculation. (b,c) By reducing the supercell size the cyano end groups bind to neighboring Cu atoms. The change in the 2HTCNPP binding energy relative to (a) is given in the inset. The positive sign indicates a reduction in binding energy. (d) Side and top view of the linear chain gas-phase model of 2HTCNPP molecules connected by single Cu atoms.

So, what drives the head-to-head coupling of the 2HTCNPP molecules and the linear chain formation since direct and substrate-mediated adsorbate−adsorbate attraction can be ruled out? As shown by several examples in the Introduction, for N-terminated molecules linking via metal adatoms has been frequently reported.[28,34,35,38−43] The Cu(111) surface is known to provide sufficient adatoms for metal−organic coordination structures.[37,38,40] To elucidate the possibility that Cu adatoms act as a linker between 2HTCNPP molecules, we performed spin-polarized DFT calculations for a gas-phase model in which we connected the two cyano groups of adjacent 2HTCNPPs by a single Cu atom to form a periodic linear chain (see Figure 4d). Similar coordination motives with adatoms have been reported before.[37,38,40,69] The structure was fully relaxed (including the lattice parameter along the chain). For the center-to-center distance of the molecules in the chain we obtain 1.963 nm. This matches very well with the measured distances in the STM experiments of 1.95 ± 0.05 nm at RT and 1.98 ± 0.05 nm at 80 K, which were acquired independently in two different experimental setups. Thus, in the observed structure of the linear chains there is enough space for interstitial Cu adatoms between the cyano groups of neighboring molecules.

DOI: 10.1021/acs.jpcc.7b08382
J. Phys. Chem. C 2017, 121, 26361−26371

Nevertheless, the close agreement for the center-to-center distance in the linear chain between our gas-phase model and the STM experiments is somewhat fortuitous, given that in the gas-phase calculations the porphyrin molecules adopt the saddle-shape conformation and not the inverted structure as on the surface (making the molecules less elongated as discussed above). In addition, the high reactivity of single Cu atoms in the gas-phase model leads to a rather short CN−Cu distance of only 1.79 Å compared to experimental values between 1.8 and 2.5 Å reported in the literature.[37,38,41,69] Both effects should lead to a shorter center-to-center distance in the gas phase than on the surface. On the other hand, since there is no underlying substrate, the Cu atoms are pulled into the molecular plane, leading to a linear CN−Cu−NC binding motif in the gas phase (see Figure 4d) instead of a triangular one on the surface where the cyano groups have to bend down in order to coordinate to the Cu atom (see Figure 3b). By forming the triangular CN−Cu−CN motif on the surface, the center-to-center distance in the chain shrinks with respect to the gas-phase model, which compensates the expansion by an increased CN−Cu distance on the surface and a more elongated rectangular shape of the 2HTCNPP in the inverted surface conformation.

For a closer look at the possible role of Cu adatoms for the head-to-head linking of the cyano-functionalized porphyrins, we expanded our previous 2HTCNPP surface calculation by including Cu adatoms. Since the experimentally measured center-to-center distance indicates that the molecular chains are not commensurate with the substrate, straightforward DFT calculations for the observed chain structures are not possible due to the large size of the corresponding unit cell. Instead, we kept our large (10 × 10) unit cell with isolated, well-separated 2HTCNPP molecules and added four Cu adatoms close to the peripheral cyano groups. The Cu adatoms prefer to occupy the fcc and hcp hollow sites on the Cu(111) surface. In view of the strong binding of the cyano groups to the Cu adatoms and the high flexibility of the porphyrin core, one might expect that by occupying different fcc and hcp hollow sites the Cu adatoms induce a variety of stable 2HTCNPP geometries with different shapes and orientations. To probe this possibility, we placed the four Cu adatoms in a variety of patterns next to and underneath the cyano groups, expecting that the porphyrin molecule will adjust to the Cu adatoms in the geometry optimization. To our surprise, the opposite happened: the porphyrin core never moved from its initial position, but the Cu adatoms were sucked underneath the cyano groups. For each of the different 2HTCNPP conformers, we obtained only one stable relaxed structure with adatoms (see Supporting Information). The inverted porphyrin structure with the hydrogens perpendicular to the close-packed Cu rows remains the energetically most favorable configuration with adatoms (see Figure 3b). Compared to the structure without adatoms, the binding energy is only reduced by 0.17 eV when calculated with respect to a gas-phase 2HTCNPP molecule, the bare Cu(111) surface, and four Cu atoms from the bulk (see Supporting Information). By using this reference, we have included the energy cost for creating the Cu adatoms. According to our DFT calculations, 0.82 eV is required for transferring one Cu atom from the bulk to the Cu(111) surface. However, if we consider experimental situations in which the Cu adatoms are basically available "for free", it would be more appropriate to calculate 2HTCNPP binding energies with respect to a Cu(111) surface with already present Cu adatoms. This would lead to 3.28 eV higher binding energy values since four Cu adatoms are involved. Thus, if we do not have to account for the energy cost to create the adatoms, incorporation of readily available Cu adatoms leads to about 3.1 eV higher 2HTCNPP binding energies compared to a surface without adatoms.

Figure 3 shows the calculated STM images for the inverted 2HTCNPP structure with and without Cu adatoms. The two upright-standing pyrrole rings give rise to a central protrusion, which is the dominating feature in the experimental STM images. Next to this protrusion, the Cu adatoms are barely visible. In particular, they do not significantly change the appearance of the porphyrin molecule. The fact that the adatoms are not visible in the STM images has been reported before also for comparable systems.[34,38]

Thus, the presence of Cu adatoms is fully compatible with the reported STM data, and they convincingly explain the head-to-head coupling of the cyano-functionalized porphyrins with the rather large center-to-center distance of about 1.95 nm. Furthermore, the CN−Cu−NC binding motif prohibits cross-linking and thus limits the chain formation to only one direction.[38] Another important factor for the observed metal−organic chains is the well-defined alignment of the molecules along the close-packed Cu rows of the Cu(111) substrate, which prohibits square linking; the latter was, e.g., observed for pyridyl porphyrins on the less reactive Au(111) surface despite the hexagonal symmetry of the substrate.[34] Overall, the general adsorption behavior of 2HTCNPP on Cu(111) is similar to the results of Klappenberger et al. for pyridyl porphyrin on the same surface.[37] One difference is, however, that for the latter system cross-linking is observed, and higher annealing temperatures up to 390 K are needed to form the chain structures. Furthermore, Ecija et al. report metal−organic chains for another pyridyl porphyrin species, which does not show cross-linking.[70] However, these structures were stable only at low temperatures and started to break apart at RT. For the system shown in our study, chains of molecules can already be found at RT, and after annealing to 350 K practically all molecules arrange in chains without any cross-linking. Therefore, 2HTCNPP on Cu(111) represents a room-temperature stable system forming surface-confined highly directional metal−organic coordinated structures. We speculate that the Cu−cyano bond is stronger than the Cu−pyridyl bond, which is a main ingredient for the stability of the 2HTCNPP molecular chains at RT.

The increased number of molecules organized in the chains after annealing to 350 K is attributed to enhanced metal−organic bond formation due to an enhanced mobility of adatoms and molecules.[22,37,38,40] Notably, at these mild annealing conditions self-metalation of the porphyrins is unlikely and does not seem to have an effect on the network formation.[18,63]

2HTCNPP/Ag(111). In order to gain deeper insight into the adsorption behavior of 2HTCNPP and in particular into the role of molecule−substrate interactions, we also investigated 2HTCNPP on Ag(111) exclusively at RT. Considering the well-established differences in the adsorption behavior of 2HTPP on Cu(111) and Ag(111), we expect a substantially different adsorption behavior also for 2HTCNPP. This is due to the fact that Ag(111) is generally considered as a less reactive surface than Cu(111) and that there is no particularly strong interaction between the nitrogen atoms of the porphyrin macrocycle and the Ag(111) surface.[16,38]

At low 2HTCNPP coverages (not shown), we observe the established indications of fast diffusing molecules on the

DOI: 10.1021/acs.jpcc.7b08382
J. Phys. Chem. C 2017, 121, 26361−26371

terraces of the Ag(111) surface, which practically form a 2D gas phase.[16,21] In addition, individual molecules adsorbed to the step edges are found. Upon increasing the coverage, the formation of long-range ordered 2D supramolecular structures is observed (see Figure 5). This adsorption behavior is

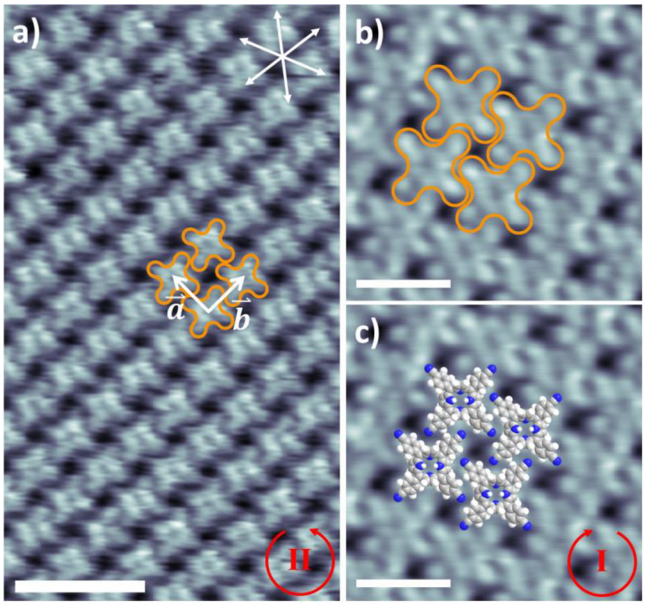

Figure 5. (a) Long-range ordered supramolecular arrangement of 2HTCNPP on Ag(111). The orange shape marks one molecule. *a* and *b* give the lattice vectors of the square unit cell. The molecules are rotated counterclockwise to the unit cell as marked by the red circle. The white arrows at the top right mark the main crystallographic substrate directions (U_{bias} = −0.55 V, I_{set} = 30 pA, scale bar = 4 nm). (b) High-resolution image of the supramolecular structure. In this contrast the phenyl groups as well as the macrocycle can be clearly distinguished (U_{bias} = −30.9 mV, I_{set} = 26 pA, scale bar = 2 nm). (c) STM image shown in (b) superimposed with molecule models giving the arrangement of molecules and groups toward each other. In this case, the molecules are rotated clockwise to the unit cell as marked by the red circle.

characteristic for systems which are dominated by molecule−molecule and not site-specific adsorbate−substrate interactions.[11,15,16,21,71] Figure 5a shows the supramolecular arrangement of a large 2HTCNPP island on Ag(111). The appearance of an individual molecule in the ordered structure is similar to that of 2HTPP on Ag(111) and will be discussed in more detail below. The orange shapes in Figure 5a indicate the porphyrin molecules; the unit cell can be described with lattice vectors a = 1.49 ± 0.02 nm and b = 1.45 ± 0.04 nm and an enclosed angle of α = 93° ± 5°. These values represent a square arrangement, similar to observations for TPPs on metal substrates.[8,12−14,16] Overall, these results suggest that the supramolecular arrangement of 2HTCNPP on Ag(111) is due to mutual stabilization via attractive intermolecular interactions;[5,10,16,21,62] the molecule−substrate interactions are rather nonsite-specific, in particular compared to the situation on Cu(111). Clearly, the adsorption behavior for 2HTCNPP on Ag(111) is substantially different than on Cu(111) where linear 1D chains are formed.

Figure 5b presents a high-resolution STM image in which the appearance of the 2HTCNPP molecules can be studied in more detail. The orange shapes serve again as a guide to the eye: the periphery of the molecule is dominated by the phenyl groups, while in the center the macrocycle is clearly visible. Overall, the appearance is very similar to the one reported for 2HTPP on Ag(111) and reflects the expected topography of 2HTCNPP well.[15] Therefore, we propose that the intramolecular conformation of 2HTCNPP on Ag(111) is the so-called "saddle shape" as depicted in Figure 1b. The evenly distributed brightness of the macrocycle in the STM image, in particular the absence of central protrusions on Ag(111), confirms a comparably undisturbed macrocycle, in contrast to the "inverted" conformation on Cu(111).

The orientation of the molecules in the square unit cell can be determined by superposition of molecular models with the high-resolution STM image as depicted in Figure 5c. While the ordered 1D 2HTCNPP chains on Cu(111) were stabilized by metal−organic coordination, a similar linking can be ruled out on Ag(111) because the orientation of cyano groups in the square arrangement does not fit to a cyano−adatom coordination. Also, to our best knowledge, there are no reports of network formation of nitrogen-terminated porphyrins on Ag(111) without codeposition of an additional metal. We therefore attribute the formation of the well-ordered stable 2D arrangement to intermolecular interactions.

To get a more detailed visualization of the orientation of molecules relative to each other and also with respect to the substrate, the square arrangement of molecules is analyzed in Figure 6. The arrangement of molecules shown in Figure 6a is

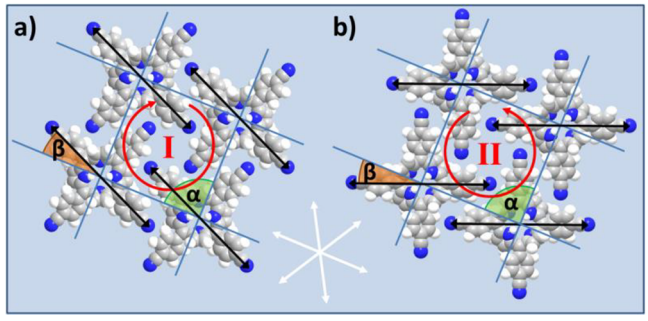

Figure 6. Model visualizing the arrangement of 2HTCNPP on Ag(111). The relevant molecular axes, marked by the black arrows, are given by two opposing phenyl rings. The blue lines mark the directions of the square unit cell (α = 90°). In (a) the molecules are rotated clockwise by β = 25 ± 5° in respect to the unit cell, while in (b) the rotation occurs counterclockwise. The red circles mark the sense of rotation. Since both structures share the same unit cell, they are chiral. The white arrows indicate the three main crystallographic directions of the Ag(111) surface.

extracted from the STM image in Figure 5c. The blue lines in Figure 6 mark the unit cell directions. An enclosed angle of approximately α = 90° is in line with the proposed square arrangement. One of the square unit cell directions coincides with one of the main crystallographic ⟨$\bar{1}$10⟩ directions of Ag(111), which are given by the white arrows. The same orientation to the substrate was also reported for the similar 2HTPP molecule on Ag(111).[15] The black arrows visualize a specific molecular axis given by the connection between two opposing phenyl legs, which was used in a previous report to quantify the azimuthal orientation within the unit cell.[15] The molecules in Figure 6a are rotated by β = 25 ± 5° clockwise to the unit cell. For such a structure, one expects organizational chirality,[19,72,73] that is, an arrangement with the same unit cell but counterclockwise rotation as in Figure 6b. The red circles indicate the sense of rotation in the respective structure.

DOI: 10.1021/acs.jpcc.7b08382
J. Phys. Chem. C 2017, 121, 26361−26371

Combining the orientation of the unit cell to the substrate with the rotation of molecules in respect to the unit cell yields six possible domains. We were able to identify four of these structures (see Figure S3 in the Supporting Information). Similar organizational chirality has been reported before for other porphyrins adsorbed on metal surfaces.[11,15,19]

The close inspection of Figure 6 yields an arrangement in which each cyano-phenyl group of a 2HTCNPP molecule faces the phenyl ring of a neighboring molecule. Evidently, the specific rotation of the phenyl rings improves the interactions of the peripheral groups. In the literature, similar structures of porphyrins on metal substrates were reported and were attributed to T-type interactions, which are typical for aromatic systems.[15−17,50] However, for 2HTCNPP the phenyl ring is terminated not by an H atom but by a cyano group. Known interactions of cyano-terminated molecules are so-called antiparallel dipole−dipole coupling and trimeric bonding.[40,41,44,48] However, the T-type like orientation of adjacent peripheral groups in Figure 6 does not suggest such interactions. Along with antiparallel dipole−dipole coupling and trimeric bonding, hydrogen bonding is stated as an intermolecular interaction motif for cyano groups.[40,41,44−46,48] Given the orientation and close distance, hydrogen bonding of cyano groups to the hydrogen atoms of the neighboring phenyl leg is reasonable. The low directionality of the hydrogen bond can be explained by the low acidity of the C−H bond.[40] The rotation angle $\beta = 25 \pm 5°$ of the molecules relative to the unit cell lattice vectors enables the interaction of each cyano group with two hydrogen atoms of an adjacent phenyl ring. Therefore, we suggest that the specific rotation of molecules is governed by intermolecular interactions, constituted by hydrogen bonds.

Since on Cu(111) metal−organic coordination via the cyano groups of 2HTCNPP was possible (see above), we wanted to study whether a similar coordination is also possible on Ag(111) by depositing metal atoms. The formation of networks after metal deposition has been reported in several studies in the literature.[38,43,45,47,69] In our study, we deposited cobalt from a metal evaporator on Ag(111) precovered with 2HTCNPP at RT. Cobalt is a promising candidate since it has been shown to form networks of nitrogen-terminated species.[28−30,36,42,43,45,47]

Figure 7a shows an STM image recorded after deposition of 0.005 ML of cobalt. While the molecular appearance (orange molecular shape) remains unchanged for most of the molecules, we identify a few brighter species marked by red molecular shape. For this species, the brightness is mainly located in the center of the molecule at the applied tunneling conditions. Since the square arrangement persists and no change in the rotation of molecules within the structures is noticed, this new species is expected to be conformational similar to 2HTCNPP.

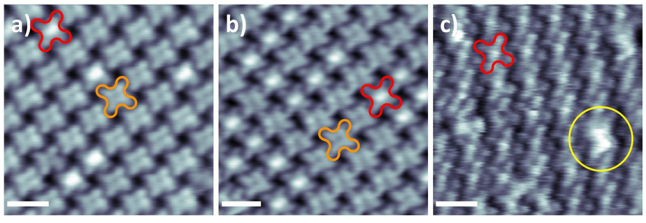

Figure 7. (a) STM image of 2HTCNPP on Ag(111) recorded after deposition of 0.005 ML of Co at RT. The species with the bright center marked by the red molecular shape accords to CoTCNPP, while the orange shape shows the unmetalated 2HTCNPP (U_{bias} = −243 mV, I_{set} = 25 pA, scale bar = 2 nm). (b) After a total deposited amount of 0.03 ML of Co the number of metalated molecules on the surface increases (U_{bias} = −240 mV, I_{set} = 26 pA, scale bar = 2 nm). (c) STM image showing full metalation of the cyano porphyrins after a total deposited amount of 0.15 ML of Co and annealing to 400 K. The bright spot in the bottom right of the island (marked yellow) accords to a Co cluster (U_{bias} = −213 mV, I_{set} = 26 pA, scale bar = 2 nm).

Upon increasing the amount of deposited Co to 0.03 ML, the number of the bright species increases (Figure 7b), indicating that the bright species is metalated CoTCNPP.[18,63,64] Room-temperature metalation of porphyrins with deposited metal has been reported before, in particular for the very similar 2HTPP. It is therefore very likely to also occur for 2HTCNPP and Co on Ag(111). Furthermore, voltage-dependent measurements show the well-investigated voltage-dependent appearance of cobalt porphyrins on Ag(111).[49] At low negative voltages, as used in Figure 7, the molecular appearance of the metalated species is dominated by a bright protrusion in the center of the molecule, while for higher negative voltages a rather longish, bright protrusion can be seen (see Figure S4 in the Supporting Information).[74]

After deposition of 0.15 ML Co, we find full metalation of 2HTCNPP on Ag(111) in Figure 7c. It should be noted that for this last deposition step mild annealing to 400 K was applied to facilitate Co diffusion. Evidently, the amount of deposited Co exceeds the stoichiometrically needed amount for full metalation (0.033 ML), yielding the formation of bright Co clusters on the surface from the "excess" material. One of these clusters is visible in the lower right part of Figure 7c (marked yellow).

Our Co codeposition experiments demonstrate metalation but provide no evidence for the formation of metal−organic network structures. Even extended annealing steps only increase the amount of metalated species. Also, reversing the deposition order, that is, deposition of 2HTCNPP onto a Co-precovered surface or Co deposition at elevated substrate temperatures, did not lead to network formation but only to the reported square structure and metalation. Deposition of Ni, which is also known to act as a linker,[39] resulted again in the same observations as for Co.

To summarize our attempts, while we found metal−organic coordinates in the form of linear 1D chains for 2HTCNPP on Cu(111) mediated by Cu adatoms, on Ag(111) no coordinated structures were found even after codeposition of Co or Ni. The linking atom itself, i.e., Cu, Co, and Ni, should not make a difference since they are chemically similar in terms of coordination compared to, e.g., Pb or Gd.[47,69] However, the role of the substrate has to be considered.[44] Fendt et al. reported that interaction to strong interacting substrates like Cu can lead to unusual structures.[40] For 2HTCNPP on Cu(111), a strong alignment of the molecules to the main crystallographic directions was observed. This molecule−substrate interaction limits the mobility and hinders the molecules to arrange into 2D supramolecular arrangements. Therefore, the formation of 1D 2HTCNPP chains, linked by Cu adatoms, is promoted. On the other hand, on Ag(111) the molecules are mobile enough to form a 2D supramolecular arrangement, which is stabilized by multiple intermolecular interactions per molecule, presumably by hydrogen bonds. Apparently, this intermolecular stabilization is strong enough to possibly prevent the formation of metal−organic networks. Within this image, the mutual stabilization within the 2D arrangement on Ag(111) realized by

DOI: 10.1021/acs.jpcc.7b08382
J. Phys. Chem. C 2017, 121, 26361−26371

multiple molecule−molecule interactions might not be thermodynamically favorable in comparison to metal coordination but might represent a kinetic obstacle, i.e., the corresponding activation barrier might not be overcome at least thermally without decomposition of the porphyrin derivatives.

These results are quite surprising because of the numerous reports in the literature about network formation with Co and molecules similar to the one used here.[34,38,41,42,45,47] However, one should note that many of the reported networks were observed at low temperatures, while our experiments were conducted at RT. Ecija et al. state that the networks observed in their work experience thermal instability.[70] In the present case of 2HTCNPP on Cu(111), the stability of the chains at RT and above is facilitated by the alignment of the molecules along densely packed Cu(111) substrate rows, which yielded the preorientation of molecules required for the linear network formation. In contrast, on Ag(111) the mobility of molecules at RT favors supramolecular arrangement by lateral stabilization.

CONCLUSIONS

We have studied and compared the adsorption behavior of 2HTCNPP on Cu(111) and Ag(111), i.e., a molecule with four cyano groups attached to the periphery. In particular on Cu(111), a novel self-assembled arrangement of 1D molecular chains without any unwanted cross-linking was observed. The linkage between the individual porphyrin building blocks is realized by Cu adatoms and metal−organic coordination. DFT gives evidence and further detailed insight into the specific linkage via Cu adatoms. In addition, the observation that individual molecules as well as the 1D porphyrin chains are oriented along one of the three main crystallographic directions of Cu(111) is comprehensibly explained by DFT as being due to a strongly attractive, site-specific interaction of the iminic nitrogens of the free−base porphyrins and the Cu substrate atoms. The assembly of practically all adsorbed 2HTCNPP molecules in 1D chains is observed after annealing the sample to 350 K due to the higher mobility of molecules. Our results on Cu(111) present a way to form RT-stable coordinate structures facilitated by the specific alignment of the molecules to the substrate. The specific role of the Cu substrate becomes even more evident by comparison with our results for 2HTCNPP on Ag(111), where a less site-specific interaction to the surface leads to the self-assembly of the molecules in 2D aggregates, which are stabilized by intermolecular interactions. The supramolecular arrangement has a square unit cell that, together with the orientation to the substrate main directions and the rotation to the lattice vectors, leads to organizational chirality. Due to the interactions between the molecules, which we attribute to hydrogen bonds, no metal−organic network formation could be found. The codeposition of metal atoms, namely, Co and Ni, only leads to metalation of 2HTCNPP at RT but not to the formation of metal-coordinated networks. Our study highlights the importance of the interplay of molecule−molecule and molecule−substrate interactions, and it proposes cyano functionalization as a powerful tool for the controlled bottom-up fabrication of supramolecular architectures.

ASSOCIATED CONTENT

Supporting Information

The Supporting Information is available free of charge on the ACS Publications website at DOI: 10.1021/acs.jpcc.7b08382.

Series of STM images showing the diffusion of an individual 2HTCNPP molecule on Cu(111). STM images at high coverages of 2HTCNPP on Cu(111) and close up of CuTCNPP species. Chiral structures found for 2HTCNPP on Ag(111). Bias-dependent appearance of CoTCNPP on Ag(111). DFT calculations on *k*-point convergence and optimized 2HTCNPP conformations on Cu(111) (PDF)

AUTHOR INFORMATION

Corresponding Author

*E-mail: hubertus.marbach@fau.de.

ORCID

Liang Zhang: 0000-0002-3446-3172
Bernd Meyer: 0000-0002-3481-8009
M. Alexander Schneider: 0000-0002-8607-3301
Hans-Peter Steinrück: 0000-0003-1347-8962
Hubertus Marbach: 0000-0002-1982-9690

Notes

The authors declare no competing financial interest.

ACKNOWLEDGMENTS

The authors gratefully acknowledge funding by the German Research Foundation (DFG) through Research Unit FOR 1878 (funCOS), Cluster of Excellence EXC 315 'Engineering of Advanced Materials' (EAM), and Collaborative Research Center SFB 953 at the Friedrich-Alexander-Universität Erlangen-Nürnberg. L.Z. thanks the Alexander von Humboldt Foundation for a research fellowship.

REFERENCES

(1) Barth, J. V. Molecular architectonic on metal surfaces. *Annu. Rev. Phys. Chem.* **2007**, *58*, 375−407.
(2) Gao, H. J.; Gao, L. Scanning tunneling microscopy of functional nanostructures on solid surfaces: Manipulation, self-assembly, and applications. *Prog. Surf. Sci.* **2010**, *85*, 28−91.
(3) Klappenberger, F. Two-dimensional functional molecular nanoarchitectures − complementary investigations with scanning tunneling microscopy and X-ray spectroscopy. *Prog. Surf. Sci.* **2014**, *89*, 1−55.
(4) Barth, J. V.; Costantini, G.; Kern, K. Engineering atomic and molecular nanostructures at surfaces. *Nature* **2005**, *437*, 671−679.
(5) De Feyter, S.; De Schryver, F. C. Two-dimensional supramolecular self-assembly probed by scanning tunneling microscopy. *Chem. Soc. Rev.* **2003**, *32*, 139−150.
(6) Jung, T. A.; Schlittler, R. R.; Gimzewski, J. K. Conformational identification of individual adsorbed molecules with the STM. *Nature* **1997**, *386*, 696−698.
(7) Auwärter, W.; Écija, D.; Klappenberger, F.; Barth, J. V. Porphyrins at interfaces. *Nat. Chem.* **2015**, *7*, 105−120.
(8) Gottfried, J. M. Surface chemistry of porphyrins and phthalocyanines. *Surf. Sci. Rep.* **2015**, *70*, 259−379.
(9) Gottfried, M.; Marbach, H. Surface-confined coordination chemistry with porphyrins and phthalocyanines: Aspects of formation, electronic structure, and reactivity. *Z. Phys. Chem.* **2009**, *223*, 53−74.
(10) Auwärter, W.; Klappenberger, F.; Weber-Bargioni, A.; Schiffrin, A.; Strunskus, T.; Wöll, C.; Pennec, Y.; Riemann, A.; Barth, J. V. Conformational adaptation and selective adatom capturing of tetrapyridyl-porphyrin molecules on a copper (111) surface. *J. Am. Chem. Soc.* **2007**, *129*, 11279−11285.
(11) Auwärter, W.; Weber-Bargioni, A.; Riemann, A.; Schiffrin, A.; Gröning, O.; Fasel, R.; Barth, J. V. Self-assembly and conformation of tetrapyridyl-porphyrin molecules on Ag(111). *J. Chem. Phys.* **2006**, *124*, 194708.

(12) Bai, Y.; Buchner, F.; Kellner, I.; Schmid, M.; Vollnhals, F.; Steinrück, H.-P.; Marbach, H.; Gottfried, J. M. Adsorption of cobalt (II) octaethylporphyrin and 2H-octaethylporphyrin on Ag(111): new insight into the surface coordinative bond. *New J. Phys.* **2009**, *11*, 125004.
(13) Barlow, D. E.; Scudiero, L.; Hipps, K. W. Scanning tunneling microscopy study of the structure and orbital-mediated tunneling spectra of cobalt (II) phthalocyanine and cobalt (II) tetraphenylporphyrin on Au (111): Mixed composition films. *Langmuir* **2004**, *20*, 4413−4421.
(14) Brede, J.; Linares, M.; Kuck, S.; Schwöbel, J.; Scarfato, A.; Chang, S. H.; Hoffmann, G.; Wiesendanger, R.; Lensen, R.; Kouwer, P. H.; et al. Dynamics of molecular self-ordering in tetraphenyl porphyrin monolayers on metallic substrates. *Nanotechnology* **2009**, *20*, 275602.
(15) Buchner, F.; Kellner, I.; Hieringer, W.; Görling, A.; Steinrück, H.-P.; Marbach, H. Ordering aspects and intramolecular conformation of tetraphenylporphyrins on Ag(111). *Phys. Chem. Chem. Phys.* **2010**, *12*, 13082−13090.
(16) Buchner, F.; Zillner, E.; Röckert, M.; Gläßel, S.; Steinrück, H.-P.; Marbach, H. Substrate-mediated phase separation of two porphyrin derivatives on Cu(111). *Chem. - Eur. J.* **2011**, *17*, 10226−10229.
(17) Lepper, M.; Zhang, L.; Stark, M.; Ditze, S.; Lungerich, D.; Jux, N.; Hieringer, W.; Steinrück, H.-P.; Marbach, H. Role of specific intermolecular interactions for the arrangement of Ni(II)-5, 10, 15, 20-tetraphenyltetrabenzoporphyrin on Cu(111). *J. Phys. Chem. C* **2015**, *119*, 19897−19905.
(18) Stark, M.; Ditze, S.; Lepper, M.; Zhang, L.; Schlott, H.; Buchner, F.; Röckert, M.; Chen, M.; Lytken, O.; Steinrück, H. P.; et al. Massive conformational changes during thermally induced self-metalation of 2H-tetrakis-(3,5-di-tert-butyl)-phenylporphyrin on Cu(111). *Chem. Commun.* **2014**, *50*, 10225−10228.
(19) Zhang, L.; Lepper, M.; Stark, M.; Lungerich, D.; Jux, N.; Hieringer, W.; Steinrück, H. P.; Marbach, H. Self-assembly and coverage dependent thermally induced conformational changes of Ni(II)-meso-tetrakis (4-tert-butylphenyl) benzoporphyrin on Cu(111). *Phys. Chem. Chem. Phys.* **2015**, *17*, 13066−13073.
(20) Yokoyama, T.; Yokoyama, S.; Kamikado, T.; Mashiko, S. Nonplanar adsorption and orientational ordering of porphyrin molecules on Au(111). *J. Chem. Phys.* **2001**, *115*, 3814.
(21) Yanagi, H.; Mukai, H.; Ikuta, K.; Shibutani, T.; Kamikado, T.; Yokoyama, S.; Mashiko, S. Molecularly resolved dynamics for two-dimensional nucleation of supramolecular assembly. *Nano Lett.* **2002**, *2*, 601−604.
(22) Buchner, F.; Xiao, J.; Zillner, E.; Chen, M.; Röckert, M.; Ditze, S.; Stark, M.; Steinrück, H.-P.; Gottfried, J. M.; Marbach, H. Diffusion, rotation, and surface chemical bond of individual 2H-tetraphenylporphyrin molecules on Cu(111). *J. Phys. Chem. C* **2011**, *115*, 24172−24177.
(23) Lepper, M.; Köbl, J.; Schmitt, T.; Gurrath, M.; de Siervo, A.; Schneider, M. A.; Steinrück, H.-P.; Meyer, B.; Marbach, H.; Hieringer, W. "Inverted" porphyrins: a distorted adsorption geometry of free-base porphyrins on Cu(111). *Chem. Commun.* **2017**, *53*, 8207−8210.
(24) Rojas, G.; Chen, X.; Bravo, C.; Kim, J.-H.; Kim, J.-S.; Xiao, J.; Dowben, P. A.; Gao, Y.; Zeng, X. C.; Choe, W. Self-assembly and properties of nonmetalated tetraphenyl-porphyrin on metal substrates. *J. Phys. Chem. C* **2010**, *114*, 9408−9415.
(25) Albrecht, F.; Bischoff, F.; Auwärter, W.; Barth, J. V.; Repp, J. Direct identification and determination of conformational response in adsorbed individual nonplanar molecular species using noncontact atomic force microscopy. *Nano Lett.* **2016**, *16*, 7703−7709.
(26) Villagómez, C. J.; Sasaki, T.; Tour, J. M.; Grill, L. Bottom-up assembly of molecular wagons on a surface. *J. Am. Chem. Soc.* **2010**, *132*, 16848−16854.
(27) Haq, S.; Hanke, F.; Dyer, M. S.; Persson, M.; Iavicoli, P.; Amabilino, D. B.; Raval, R. Clean coupling of unfunctionalized porphyrins at surfaces to give highly oriented organometallic oligomers. *J. Am. Chem. Soc.* **2011**, *133*, 12031−12039.
(28) Reichert, J.; Marschall, M.; Seufert, K.; Ecija, D.; Auwärter, W.; Arras, E.; Klyatskaya, S.; Ruben, M.; Barth, J. V. Competing interactions in surface reticulation with a prochiral dicarbonitrile linker. *J. Phys. Chem. C* **2013**, *117*, 12858−12863.
(29) Stepanow, S.; Lin, N.; Barth, J. V. Modular assembly of low-dimensional coordination architectures on metal surfaces. *J. Phys.: Condens. Matter* **2008**, *20*, 184002.
(30) Clair, S.; Pons, S.; Brune, H.; Kern, K.; Barth, J. V. Mesoscopic metallosupramolecular texturing by hierarchic assembly. *Angew. Chem., Int. Ed.* **2005**, *44*, 7294−7297.
(31) Classen, T.; Fratesi, G.; Costantini, G.; Fabris, S.; Stadler, F. L.; Kim, C.; de Gironcoli, S.; Baroni, S.; Kern, K. Templated growth of metal-organic coordination chains at surfaces. *Angew. Chem., Int. Ed.* **2005**, *44*, 6142−6145.
(32) Lin, N.; Dmitriev, A.; Weckesser, J.; Barth, J. V.; Kern, K. Real-time single-molecule imaging of the formation and dynamics of coordination compounds. *Angew. Chem., Int. Ed.* **2002**, *41*, 4779−4783.
(33) Ecija, D.; Vijayaraghavan, S.; Auwärter, W.; Joshi, S.; Seufert, K.; Aurisicchio, C.; Bonifazi, D.; Barth, J. V. Two-dimensional short-range disordered crystalline networks from flexible molecular modules. *ACS Nano* **2012**, *6*, 4258−4265.
(34) Li, Y.; Xiao, J.; Shubina, T. E.; Chen, M.; Shi, Z.; Schmid, M.; Steinrück, H. P.; Gottfried, J. M.; Lin, N. Coordination and metalation bifunctionality of Cu with 5,10,15,20-tetra(4-pyridyl)porphyrin: toward a mixed-valence two-dimensional coordination network. *J. Am. Chem. Soc.* **2012**, *134*, 6401−6408.
(35) Vijayaraghavan, S.; Ecija, D.; Auwärter, W.; Joshi, S.; Seufert, K.; Drach, M.; Nieckarz, D.; Szabelski, P.; Aurisicchio, C.; Bonifazi, D.; et al. Supramolecular assembly of interfacial nanoporous networks with simultaneous expression of metal-organic and organic-bonding motifs. *Chem. - Eur. J.* **2013**, *19*, 14143−14150.
(36) El Garah, M.; Ciesielski, A.; Marets, N.; Bulach, V.; Hosseini, M. W.; Samori, P. Molecular tectonics based nanopatterning of interfaces with 2D metal-organic frameworks (MOFs). *Chem. Commun.* **2014**, *50*, 12250−12253.
(37) Klappenberger, F.; Weber-Bargioni, A.; Auwärter, W.; Marschall, M.; Schiffrin, A.; Barth, J. V. Temperature dependence of conformation, chemical state, and metal-directed assembly of tetrapyridyl-porphyrin on Cu(111). *J. Chem. Phys.* **2008**, *129*, 214702.
(38) Heim, D.; Ecija, D.; Seufert, K.; Auwärter, W.; Aurisicchio, C.; Fabbro, C.; Bonifazi, D.; Barth, J. V. Self-assembly of flexible one-dimensional coordination polymers on metal surfaces. *J. Am. Chem. Soc.* **2010**, *132*, 6783−6790.
(39) Abdurakhmanova, N.; Tseng, T. C.; Langner, A.; Kley, C. S.; Sessi, V.; Stepanow, S.; Kern, K. Superexchange-mediated ferromagnetic coupling in two-dimensional Ni-TCNQ networks on metal surfaces. *Phys. Rev. Lett.* **2013**, *110*, 027202.
(40) Fendt, L. A.; Stöhr, M.; Wintjes, N.; Enache, M.; Jung, T. A.; Diederich, F. Modification of supramolecular binding motifs induced by substrate registry: formation of self-assembled macrocycles and chain-like patterns. *Chem. - Eur. J.* **2009**, *15*, 11139−11150.
(41) Gottardi, S.; Müller, K.; Moreno-López, J. C.; Yildirim, H.; Meinhardt, U.; Kivala, M.; Kara, A.; Stöhr, M. Cyano-functionalized triarylamines on Au(111): competing intermolecular versus molecule/substrate interactions. *Adv. Mater. Interfaces* **2014**, *1*, 1300025.
(42) Henningsen, N.; Rurali, R.; Limbach, C.; Drost, R.; Pascual, J.; Franke, K. Site-dependent coordination bonding in self-assembled metal−organic networks. *J. Phys. Chem. Lett.* **2010**, *2*, 55−61.
(43) Schlickum, U.; Decker, R.; Klappenberger, F.; Zoppellaro, G.; Klyatskaya, S.; Ruben, M.; Silanes, I.; Arnau, A.; Kern, K.; Brune, H. Metal-organic honeycomb nanomeshes with tunable cavity size. *Nano Lett.* **2007**, *7*, 3813−3817.
(44) Mohnani, S.; Bonifazi, D. Supramolecular architectures of porphyrins on surfaces: The structural evolution from 1D to 2D to 3D to devices. *Coord. Chem. Rev.* **2010**, *254*, 2342−2362.
(45) Schlickum, U.; Decker, R.; Klappenberger, F.; Zoppellaro, G.; Klyatskaya, S.; Auwärter, W.; Neppl, S.; Kern, K.; Brune, H.; Ruben, M.; et al. Chiral kagomé lattice from simple ditopic molecular bricks. *J. Am. Chem. Soc.* **2008**, *130*, 11778−11782.
(46) Stöhr, M.; Boz, S.; Schar, M.; Nguyen, M. T.; Pignedoli, C. A.; Passerone, D.; Schweizer, W. B.; Thilgen, C.; Jung, T. A.; Diederich, F.

DOI: 10.1021/acs.jpcc.7b08382
J. Phys. Chem. C 2017, 121, 26361−26371

Self-assembly and two-dimensional spontaneous resolution of cyano-functionalized [7]helicenes on Cu(111). *Angew. Chem., Int. Ed.* **2011**, *50*, 9982−9986.
(47) Urgel, J. I.; Ecija, D.; Auwärter, W.; Stassen, D.; Bonifazi, D.; Barth, J. V. Orthogonal insertion of lanthanide and transition-metal atoms in metal-organic networks on surfaces. *Angew. Chem., Int. Ed.* **2015**, *54*, 6163−6167.
(48) Yokoyama, T.; Yokoyama, S.; Kamikado, T.; Okuno, Y.; Mashiko, S. Selective assembly on a surface of supramolecular aggregates with controlled size and shape. *Nature* **2001**, *413*, 619−621.
(49) Buchner, F.; Warnick, K.-G.; Wölfle, T.; Görling, A.; Steinrück, H.-P.; Hieringer, W.; Marbach, H. Chemical fingerprints of large organic molecules in scanning tunneling microscopy: Imaging adsorbate−substrate coupling of metalloporphyrins. *J. Phys. Chem. C* **2009**, *113*, 16450−16457.
(50) Brede, J.; Linares, M.; Lensen, R.; Rowan, A. E.; Funk, M.; Bröring, M.; Hoffmann, G.; Wiesendanger, R. Adsorption and conformation of porphyrins on metallic surfaces. *J. Vac. Sci. Technol., B: Microelectron. Nanometer Struct.* **2009**, *27*, 799.
(51) Diller, K.; Klappenberger, F.; Marschall, M.; Hermann, K.; Nefedov, A.; Wöll, C.; Barth, J. V. Self-metalation of 2H-tetraphenylporphyrin on Cu(111): an x-ray spectroscopy study. *J. Chem. Phys.* **2012**, *136*, 014705.
(52) Horcas, I.; Fernández, R.; Gomez-Rodriguez, J.; Colchero, J.; Gómez-Herrero, J.; Baro, A. WSXM: a software for scanning probe microscopy and a tool for nanotechnology. *Rev. Sci. Instrum.* **2007**, *78*, 013705.
(53) Giannozzi, P.; Baroni, S.; Bonini, N.; Calandra, M.; Car, R.; Cavazzoni, C.; Ceresoli, D.; Chiarotti, G. L.; Cococcioni, M.; Dabo, I.; et al. QUANTUM ESPRESSO: a modular and open-source software project for quantum simulations of materials. *J. Phys.: Condens. Matter* **2009**, *21*, 395502.
(54) Perdew, J. P.; Burke, K.; Ernzerhof, M. Generalized gradient approximation made simple. *Phys. Rev. Lett.* **1996**, *77*, 3865−3868.
(55) Grimme, S.; Antony, J.; Ehrlich, S.; Krieg, H. A consistent and accurate ab initio parametrization of density functional dispersion correction (DFT-D) for the 94 elements H-Pu. *J. Chem. Phys.* **2010**, *132*, 154104.
(56) Grimme, S.; Ehrlich, S.; Goerigk, L. Effect of the damping function in dispersion corrected density functional theory. *J. Comput. Chem.* **2011**, *32*, 1456−1465.
(57) Vanderbilt, D. Soft self-consistent pseudopotentials in a generalized eigenvalue formalism. *Phys. Rev. B: Condens. Matter Mater. Phys.* **1990**, *41*, 7892−7895.
(58) Within the Γ-point approximation, binding energies are off by up to 0.6 eV, and a wrong ordering of the relative stability of the different porphyrin binding modes is predicted. See Supporting Information.
(59) Kováčik, R.; Meyer, B.; Marx, D. F centers versus dimer vacancies on ZnO surfaces: Characterization by STM and STS calculations. *Angew. Chem., Int. Ed.* **2007**, *46*, 4894−4897.
(60) Lucas, R.; Vergnaud, J.; Teste, K.; Zerrouki, R.; Sol, V.; Krausz, P. A facile and rapid iodine-catalyzed meso-tetraphenylporphyrin synthesis using microwave activation. *Tetrahedron Lett.* **2008**, *49*, 5537−5539.
(61) Asano, N.; Uemura, S.; Kinugawa, T.; Akasaka, H.; Mizutani, T. Synthesis of biladienone and bilatrienone by coupled oxidation of tetraarylporphyrins. *J. Org. Chem.* **2007**, *72*, 5320−5326.
(62) Auwärter, W.; Weber-Bargioni, A.; Brink, S.; Riemann, A.; Schiffrin, A.; Ruben, M.; Barth, J. V. Controlled metalation of self-assembled porphyrin nanoarrays in two dimensions. *ChemPhysChem* **2007**, *8*, 250−254.
(63) Xiao, J.; Ditze, S.; Chen, M.; Buchner, F.; Stark, M.; Drost, M.; Steinrück, H.-P.; Gottfried, J. M.; Marbach, H. Temperature-dependent chemical and structural transformations from 2H-tetraphenylporphyrin to Copper(II)-tetraphenylporphyrin on Cu(111). *J. Phys. Chem. C* **2012**, *116*, 12275−12282.
(64) Marbach, H. Surface-mediated in situ metalation of porphyrins at the solid-vacuum interface. *Acc. Chem. Res.* **2015**, *48*, 2649−2658.
(65) Ditze, S.; Stark, M.; Drost, M.; Buchner, F.; Steinrück, H.-P.; Marbach, H. Activation energy for the self-metalation reaction of 2H-tetraphenylporphyrin on Cu(111). *Angew. Chem., Int. Ed.* **2012**, *51*, 10898−10901.
(66) Grimme, S. Do special noncovalent pi-pi stacking interactions really exist? *Angew. Chem., Int. Ed.* **2008**, *47*, 3430−3434.
(67) Sinnokrot, M. O.; Sherrill, C. D. High-accuracy quantum mechanical studies of π-π interactions in benzene dimers. *J. Phys. Chem. A* **2006**, *110*, 10656−10668.
(68) Tseng, T.-C.; Urban, C.; Wang, Y.; Otero, R.; Tait, S. L.; Alcamí, M.; Écija, D.; Trelka, M.; Gallego, J. M.; Lin, N.; et al. Charge-transfer-induced structural rearrangements at both sides of organic/metal interfaces. *Nat. Chem.* **2010**, *2*, 374−379.
(69) Lyu, G.; Zhang, R.; Zhang, X.; Nian Liu, P.; Lin, N. On-surface assembly of low-dimensional Pb-coordinated metal−organic structures. *J. Mater. Chem. C* **2015**, *3*, 3252−3257.
(70) Ecija, D.; Marschall, M.; Reichert, J.; Kasperski, A.; Nieckarz, D.; Szabelski, P.; Auwärter, W.; Barth, J. V. Dynamics and thermal stability of surface-confined metal−organic chains. *Surf. Sci.* **2015**, *643*, 91−97.
(71) Besenbacher, F. Scanning tunnelling microscopy studies of metal surfaces. *Rep. Prog. Phys.* **1996**, *59*, 1737.
(72) Ernst, K. H. Molecular chirality at surfaces. *Phys. Status Solidi B* **2012**, *249*, 2057−2088.
(73) Raval, R. Chiral expression from molecular assemblies at metal surfaces: Insights from surface science techniques. *Chem. Soc. Rev.* **2009**, *38*, 707−721.
(74) Scudiero, L.; Barlow, D. E.; Hipps, K. W. Physical properties and metal ion specific scanning tunneling microscopy images of metal (II) tetraphenylporphyrins deposited from vapor onto gold (111). *J. Phys. Chem. B* **2000**, *104*, 11899−11905.

DOI: 10.1021/acs.jpcc.7b08382
J. Phys. Chem. C 2017, 121, 26361−26371